Pol. J. Environ. Stud. Vol. XX, No. X (XXXX), 1-16
DOI: *10.15244/pjoes/231056* ONLINE PUBLICATION DATE: 2026-11-03

Original Research

Comparison of Hydrochemical Characteristics of Groundwater in the Qihe River Alluvial Fan of North China over the Past 35 Years

Chao Bian[1, 2], Huaisheng Zhang[1, 2, 4]*, Jinwei Liu[2], Weiwei Shi[3], Dandan Liu[2], Yonggao Lyu[2]**

[1]Hebei Province Collaborative Innovation Center for Sustainable Utilization of Water Resources and Optimization of Industrial Structure, Hebei GEO University, Shijiazhuang 050031, China
[2]Center for Hydrogeology and Environmental Geology Survey, China Geological Survey, Tianjin 300309, China
[3]The Prevent and Control Center for the Geological Disaster of Henan Geological Bureau, Zhengzhou 450000, China
[4]State Key Laboratory of Biogeography and Environmental Geology, Wuhan 430078, China

Received: 25 March 2026
Accepted: 12 August 2026

Abstract

Groundwater resources play a crucial role in socioeconomic development and domestic water use in piedmont alluvial plain areas. In this study, the Qihe River alluvial fan (QRAF) was selected as a representative area to investigate the evolutionary patterns of shallow groundwater chemistry in the North China Plain (NCP). Based on shallow groundwater monitoring data collected during the wet seasons of 1983 and 2017, the spatiotemporal trends in chemical characteristics and their influencing factors in shallow groundwater in the QRAF were studied using multi-hydrochemical and statistical methods. The results showed that the groundwater in the QRAF was generally weakly alkaline, and groundwater quality has generally deteriorated over time. In particular, the concentrations of Cl^- and NO_3^-, two important indicators of water quality and pollution, increased significantly in 2017 compared with 1983. Although the groundwater chemical types were still dominated by HCO_3-Ca and HCO_3-Ca·Mg types, significant changes occurred along the middle to outer edge of the fan between 1983 and 2017, especially in the low-lying areas along the Weihe River. In 1983, the groundwater chemical composition was primarily controlled by natural processes such as water-rock interaction, whereas in 2017 it was additionally affected by anthropogenic activities, resulting in a more complex hydrochemical driving mechanism. The research findings can provide a reference for groundwater safety and protection management in the QRAF and other similar areas in the world.

Keywords: alluvial fan, controlling factors, groundwater, hydrochemistry, North China Plain (NCP), temporal variation

*e-mail: zhanghuaisheng@mail.cgs.gov.cn
**e-mail: 116593545@qq.com
0000-0002-5579-4608

© 2026 This article is licensed under a Creative Commons Attribution-NonCommercial 4.0 International (CC BY-NC 4.0)

Introduction

As the most ubiquitous source of liquid freshwater globally [1], groundwater is abundant and widely distributed, and its use underpins a huge range of human activities as well as important ecosystems [2-4]. In general, temporal and spatial variations in groundwater hydrochemistry depend on geogenic factors such as recharge sources, flow paths, water-rock interactions, and hydrogeological settings [5, 6]. In recent decades, anthropogenic activities such as industrial and agricultural production have accelerated changes in groundwater quality [7, 8], leading to complex and diverse water quality issues [9, 10] that demand urgent global attention. Therefore, understanding temporal and spatial variations in groundwater quality has become essential for effective groundwater management and sustainable use [11].

Groundwater chemistry is naturally governed by various physical and chemical reactions among water, gases, and rocks during the hydrological cycle. Key physical processes include mixing, evaporation and concentration. In areas with multiple sources of supply, the different chemical compositions of water from different sources, especially sewage, can cause significant changes in the chemical composition of the mixed water. Evaporation and concentration are additional physical processes that influence the evolution of water quality, and strong evaporation will cause saltwater to be distributed over a large area, especially in arid and semi-arid regions with shallow groundwater tables [12]. The dissolution of carbonate, silica rock and evaporated rock salt or other water-rock interactions in the water cycle greatly affect the groundwater quality [13]. Furthermore, studies have revealed that cation exchange and adsorption in the Quaternary aquifer of the plain area, which is dominated by clay or silt, largely control changes in cation concentrations in groundwater [12, 14]. In addition to natural factors, the intensifying human activities in recent years have led to an influx of pollutants into the aquifer, altering the natural groundwater quality and resulting in the deterioration of groundwater in numerous regions [15]. An effective way to mitigate the ongoing deterioration of groundwater quality is to assess the relative influence of natural and anthropogenic factors on groundwater quality in different periods in typical regions and analyze the causes of hydrochemical evolution.

The North China Plain (NCP), situated east of the Taihang Mountains, south of the Yanshan Mountains, and north of the Yellow River, is a major grain-producing area in China [16]. Currently, groundwater in the NCP faces two major challenges: water scarcity and quality deterioration, with shallow groundwater being particularly affected by human activities [17]. In the NCP, human activities mainly involve urbanization and agricultural activities, and previous studies on groundwater quality evolution have primarily focused on the central plain regions [18-21]. However, the less-studied piedmont alluvial slope area is one of the main groundwater recharge areas in the NCP [22], with coarse formation particles, strong vertical continuity, a single- or double-layer structure, and strong infiltration recharge and storage conditions. The inclined plain of foremountain alluvium and diluvium experiences frequent human activity [23], lies at the intersection of agriculture, forestry, and animal husbandry, and features diverse land use types. The high permeability of piedmont soils facilitates the infiltration of various anthropogenic pollutants originating from both point and non-point sources related to human activities into aquifers. This permeability also aids the movement of pollutants along groundwater flow paths [6]. Once groundwater becomes contaminated, it is extremely difficult to remediate. Liu et al. [22] used stable isotopes and main ions to analyze the recharge mechanism of alluvial fan aquifers in the piedmont area of the southern Taihang Mountains, and found that the shallow groundwater level in the Shahe River alluvial fan dropped significantly due to excessive mining, which affected the recharge conditions of the aquifers. In addition, Zhang et al. [24] assessed groundwater quality of the Hutuo River alluvial-pluvial fan region in the NCP using a water quality index and showed that 53.09 % of NO_3^-, 18.52 % of SO_4^{2-} and 83.95 % of TH samples surpassed the Grade III standard for groundwater quality in China (GB/T 14848-2017). Therefore, it is necessary to explore the groundwater chemical characteristics of typical piedmont alluvial fans in North China and analyze long-term changes in their hydrological and chemical characteristics, in order to help prevent further water quality deterioration.

In this study, the Qihe River alluvial fan (QRAF), located in the piedmont alluvial-proluvial inclined plain of North China, was selected as the study area. Based on data collected through field investigation and sampling, hydrogeochemical and statistical methods were used to compare and analyze the shallow groundwater-quality characteristics in 1983 and 2017, and to reveal the hydrochemical evolution patterns and controlling factors of groundwater under the combined effects of natural processes and anthropogenic disturbance during different periods. It is expected to provide a useful reference for supporting sustainable groundwater exploitation and management in the QRAF and understanding the mechanism of groundwater chemical evolution in the NCP.

Materials and Methods

Study Area

The Qihe River alluvial fan (QRAF) is situated in the southern part of the NCP, spanning from 114°04′ to 114°26′E and 35°30′ to 35°49′N. It is one of the piedmont alluvial fans formed by rivers originating from the Taihang Mountains (Fig. 1a)). It stretches from

the fan apex in the west to the fan toe in the east, bounded by the Weihe River to the south and the outskirts of Hebi City to the north, encompassing most of Qibin District (Hebi City), Qixian County, and the Weixian area in western Xunxian County. The terrain generally slopes from the highlands in the northwest to the lowlands in the southeast, forming a step-like gradient. Since the Cenozoic, the Taihang Mountains have experienced continuous uplift while the NCP has subsided, providing the internal geodynamic conditions for the region's geomorphic development, while erosion and sediment accumulation by the Qihe River serve as the external dynamic forces driving geomorphic evolution. Overall, the five geomorphic units in the study area, namely low mountains and hills, sloping proluvial deposits, the alluvial-proluvial fan, the fan-front depression, and the interfan transition zone, are clearly developed and zoned (Fig. 1b)), making it a typical representative of piedmont alluvial-proluvial fans in North China.

The study area experiences a temperate continental monsoon climate, characterized by four distinct seasons, abundant sunshine, and significant temperature variations. The annual average temperature is 14.2-15.5ºC [25], and the annual sunshine duration is 1787.2-2566.7 h. The spatial and temporal distribution of precipitation is extremely uneven, and precipitation decreases from west to east. The rainfall is concentrated during the flood season, with an average annual precipitation of 674.8 mm and an average annual evaporation of 1700 mm, including approximately 520 mm of surface evaporation.

Neogene and Paleogene strata are exposed at depths below 40 m in the low mountain and hill regions in the northern part of the study area, and the Qingyangkou Fault runs through the alluvial fan in the western region. According to the north-south hydrogeological profile (Fig. 2), the lithology of the QRAF is limestone in the north, siltstone in the south from the Qingyangkou Fault to Zhangzhuang, and a clay-sandstone interbedded structure in the south to the fan margin. The main water-rich rock formation in the study area is sandstone. From the fan-front area through the middle fan to the fan margin, the thickness of clay layers gradually increases, and the Quaternary aquifer gradually transitions from a single coarse-grained porous aquifer to a multilayer composite aquifer, representing a typical shallow groundwater circulation pattern in a piedmont alluvial-proluvial fan.

Groundwater Sampling

57 representative shallow groundwater sampling points were selected in the study area during the wet season in September 2017. Prior to sampling, a volume of groundwater exceeding three times the borehole capacity was purged to eliminate the influence of stagnant water on the collected samples. The pH and electrical conductivity (EC) parameters of the pumped water were monitored on site, and groundwater samples were collected once these parameters stabilized. Each group of samples was collected in 500 mL polyethylene bottles, and the collected samples were unfiltered and used directly for major ion analysis. All bottles were thoroughly rinsed with the target groundwater at least three times prior to sampling. Groundwater samples were stored in a 4ºC cooler immediately after collection until they were sent to the laboratory for analysis.

In order to study the variation of shallow groundwater quality in the QRAF over the past 35 years, 9 shallow groundwater samples collected during the wet season in

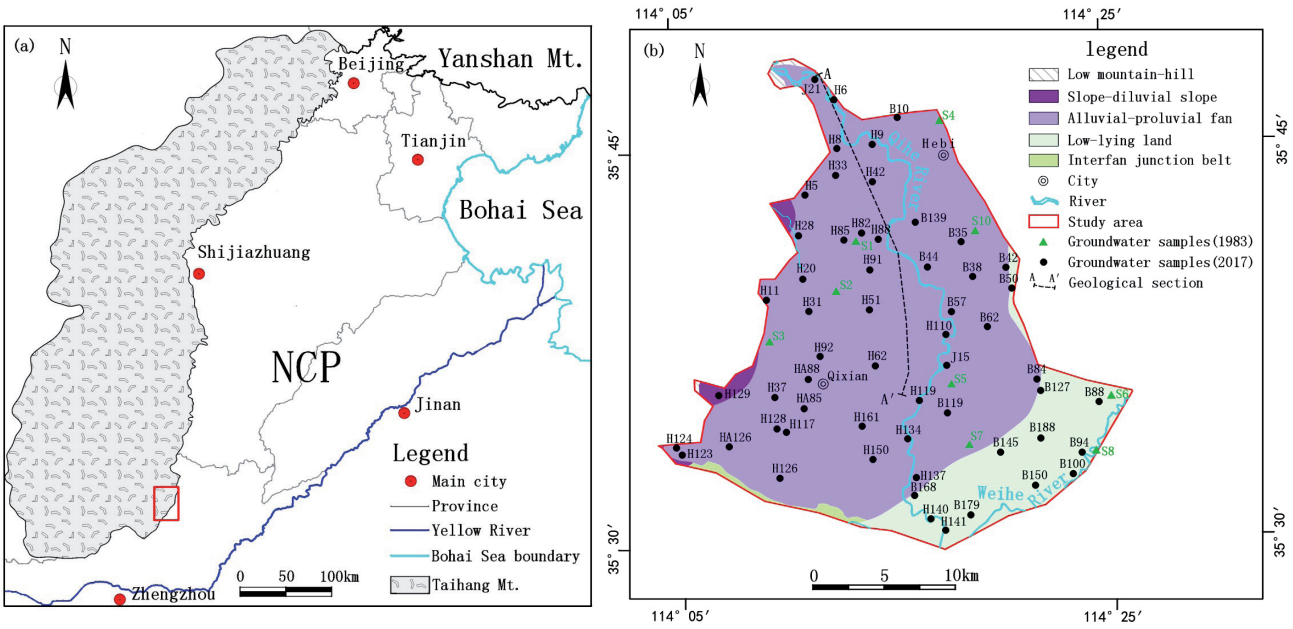


Fig. 1. Geomorphic types and spatial distribution of sampling sites in the study area.

1983 were selected for comparative analysis according to the "Report of Regional Hydrogeological Survey (Hebi)" compiled by the First Hydrogeology Team of the Henan Provincial Bureau of Geology and Mineral Resources in October 1985. The locations of sampling points are shown in Fig. 1b).

Physicochemical Analysis

Laboratory analyses of the water samples collected in 2017 were conducted at the Center for Hydrogeology and Environmental Geology Survey, China Geological Survey, following the geological and mineral industry standard "Methods for Groundwater Quality Analysis" (DZ/T 0064-93). Basic parameters, such as pH and EC, were measured in situ using a portable multiparameter device (HACH multi HQ40d, Colorado, USA), which was calibrated prior to sampling to ensure measurement accuracy. The total dissolved solids (TDS) were measured using a weighing technique. Total hardness (TH), CO_3^{2-} and HCO_3^- were determined using titration methods. Major cations including K^+, Na^+, Ca^{2+} and Mg^{2+} were measured using a flame atomic absorption spectrometer (Analytic Jena ContrAA300, Thuringia, Germany). Major anions, including Cl^-, SO_4^{2-} and NO_3^-, were measured using ion chromatographs (Metrohm 883i, Herisau, Switzerland). Groundwater quality data from 1983 were obtained from the "List of Water Quality Analysis Results" appended to the "Report of Regional Hydrogeological Survey (Hebi)", and the parameters included pH, TH, TDS, K^+, Na^+, Ca^{2+}, Mg^{2+}, HCO_3^-, SO_4^{2-}, Cl^- and NO_3^-. The analytical methods for the 1983 water-quality parameters followed the 1974 "Operating Procedures for Groundwater Quality Analysis (Revised Edition)" issued by the Ministry of Geology, which was the predecessor of DZ/T 0064-93. The two methods are broadly consistent in the core analytical principles for major groundwater cations and anions and in sampling requirements; therefore, the 1983 and 2017 water-quality datasets are highly comparable.

The analytical precision of ion measurements was assessed by calculating ionic balance errors using Eq. (1) [26]. The CBE values of water samples in 1983 were all in the interval [0 - ±5 %]. In 2017, the mean CBE was 1.96%, with 97% of the samples in the interval [0 - ±5 %] and 3 % in the interval [±5 - ±6 %], indicating that the quality of the resulting data was sufficient for hydrochemical analysis [27, 28]. Therefore, no outliers were excluded from the 1983 and 2017 water-quality datasets, and all samples were used for the hydrochemical analysis of the study area.

$$\%CBE = \left(\sum ce_i^+ - \sum ce_j^-\right) / \left(\sum ce_i^+ + \sum ce_j^-\right) \times 100 \quad (1)$$

where ce_i^+ and ce_j^-, which are expressed in meq/L, represent specific cation and anion charge concentrations, respectively [6].

Analysis Methods

To determine the hydrochemical characteristics and formation mechanisms of groundwater in 1983 and 2017, statistical and integrated hydrochemical analysis methods were applied. First, IBM SPSS and OriginPro were used for the statistical analysis of the data. Second, the Shukarev classification method was employed to categorize groundwater types, and the results were visualized using MapGIS software. Then, to investigate the primary controlling factors of groundwater chemistry in the QRAF, Gibbs diagrams, end-member diagrams, and ion-ratio relationships were utilized.

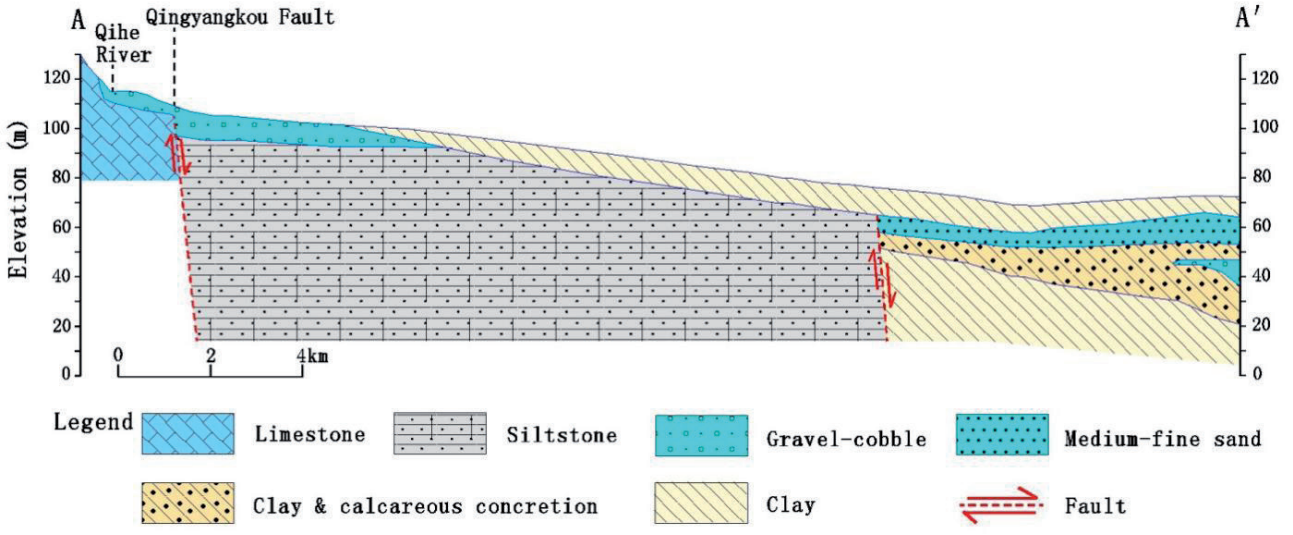


Fig. 2. Schematic diagram of the hydrogeological cross-section in the QRAF.

Table 1. Statistics of main chemical components in groundwater.

Parameters	1983					2017				
	Max	Min	Mean	SD	CV (%)	Max	Min	Mean	SD	CV (%)
K^+ (mg/L)	20.82	0.90	5.34	6.44	120.60	18.70	0.32	1.80	3.00	166.67
Na^+ (mg/L)	187.38	8.10	48.08	58.01	120.65	339.00	5.79	44.54	59.58	133.77
Ca^{2+} (mg/L)	139.10	52.30	78.59	26.64	33.90	326.00	55.45	126.34	53.60	42.43
Mg^{2+} (mg/L)	54.70	14.20	28.20	14.46	51.28	132.00	18.65	44.49	20.37	45.79
Cl^- (mg/L)	104.60	7.10	33.09	34.21	103.38	350.04	9.09	78.93	81.50	103.26
SO_4^{2-} (mg/L)	243.50	14.90	89.44	81.93	91.60	361.00	13.13	90.12	77.59	86.10
HCO_3^- (mg/L)	567.50	219.70	324.90	105.20	32.38	773.00	209.98	390.40	109.66	28.09
NO_3^- (mg/L)	200.30	0.10	24.06	66.17	275.02	309.60	0.01	60.46	69.81	115.46
TDS (mg/L)	930	290	473.33	240.52	50.81	1620	173	643.81	353.93	54.97
TH (mg/L)	488.29	214.32	312.53	101.36	32.43	1017.77	254.84	498.68	182.26	36.55
pH	7.90	6.95	7.46	0.33	4.42	8.19	6.32	7.51	0.36	4.79

Results and Discussion

Changes in Chemical Composition Characteristics of Groundwater

The statistical results of the main chemical components of groundwater in the QRAF are shown in Table 1. The overall concentrations of major ions in groundwater followed the same order in both 1983 and 2017, namely: HCO_3^->SO_4^{2-}>Cl^->NO_3^- for anions and Ca^{2+}>Na^+>Mg^{2+}>K^+ for cations. The groundwater in both 1983 and 2017 exhibited similar pH values, indicating moderately to weakly alkaline conditions. The pH in 1983 ranged from 6.95 to 7.90, with an average value of 7.46, whereas that in 2017 ranged from 6.32 to 8.19, with an average value of 7.51. Their coefficients of variation (CVs) were small, indicating relatively stable pH conditions. In contrast, the concentrations of Cl^- and NO_3^-, which are two important indicators of water quality and pollution, changed significantly. The concentrations of Cl^- in 1983 and 2017 ranged from 7.10 to 104.60 mg/L and from 9.09 to 350.04 mg/L, with average values of 33.09 and 78.93 mg/L, respectively. NO_3^- concentrations in 1983 and 2017 ranged from 0.10 to 200.30 and from 0.01 to 309.60 mg/L, with average values of 24.06 and 60.46 mg/L, respectively. The notably higher levels of NO_3^- in 2017 indicate a growing impact of anthropogenic activities on groundwater quality over the past 35 years.

TDS concentrations in 1983 and 2017 ranged from 290 to 930 and from 173 to 1620 mg/L, with average values of 473.33 and 643.81 mg/L, respectively. Similarly, the levels of TH ranged from 214.32 to 488.29 mg/L and from 254.84 to 1017.77 mg/L, with mean values of 312.53 and 498.68 mg/L. According to the classification standards based on TDS and TH [29], all groundwater samples in 1983 were categorized as hard-fresh water. However, groundwater in 2017 was mostly classified as hard-fresh water (85.96 %), followed by hard-brackish water (14.04 %), as shown in Fig. 3a). Furthermore, all of the groundwater samples in 1983 were plotted below the TIS = 40 meq/L line, indicating low TIS values [30]. By contrast, comparatively high TIS values between 40 and 60 meq/L were observed in 10.53% of the groundwater samples in 2017 (Fig. 3b)).

Spatial Pattern of TDS

Total dissolved solids (TDS) in groundwater is a key parameter used to characterize hydrogeochemical processes and regional geochemical conditions, as it reflects the cumulative concentration of dissolved constituents and indicates the long-term evolution of groundwater hydrochemistry [31, 32]. As shown in Fig. 4, the majority of groundwater points in 1983 exhibited low TDS concentrations, with only two relatively high values (760 and 930 mg/L) observed in the southeastern ancient channel depression, where reduced groundwater runoff and enhanced evaporation likely contributed to elevated TDS. By contrast, groundwater TDS levels in 2017 showed a general increase, with pronounced high values in the lower reaches of the Qihe River, along the Weihe River, and within the ancient river depression of the southeastern area of the QRAF. Notably, the maximum recorded value reached 1620 mg/L.

Hydrochemical Evolution Characteristics

According to the Shukarev classification method [33, 34], the hydrochemical types in the study area underwent significant changes from 1983 to 2017 (Fig. 5). In 1983, the predominant groundwater types were HCO_3-Ca and HCO_3-Ca·Mg types, while HCO_3·SO_4-

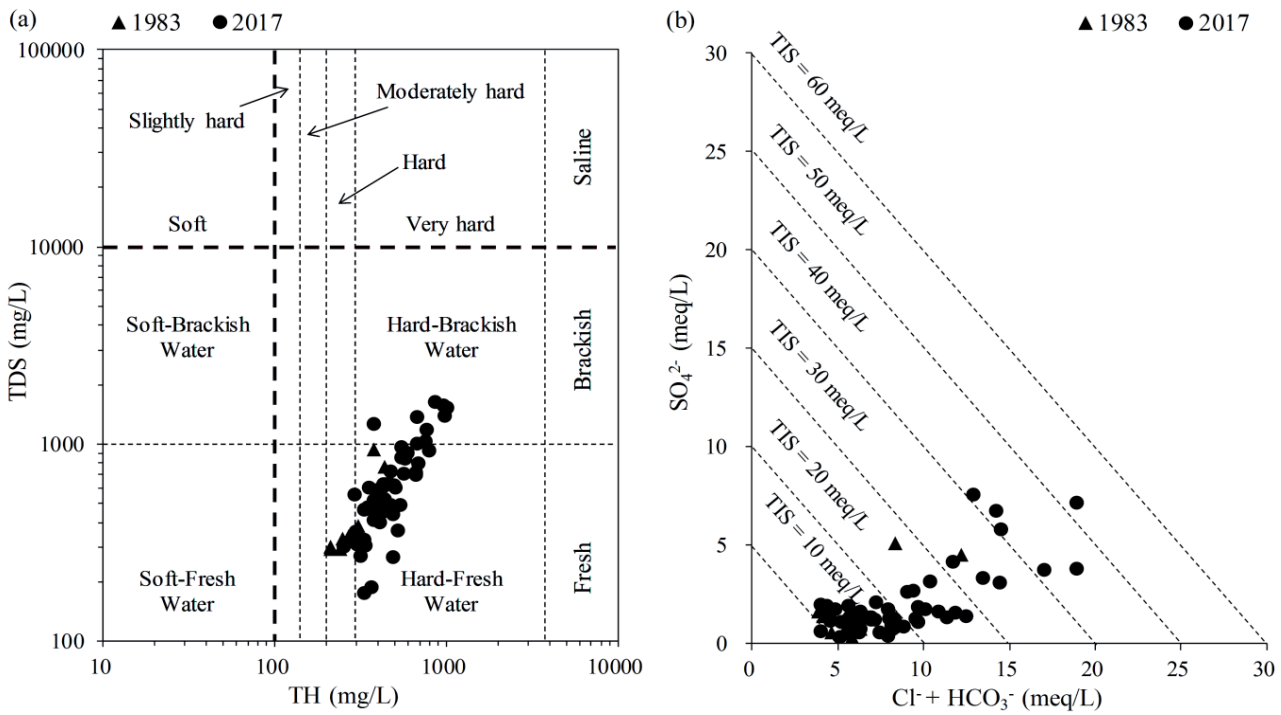


Fig. 3. Relationships between a) TDS and TH and b) SO_4^{2-} and $Cl^- + HCO_3^-$ in groundwater of the QRAF.

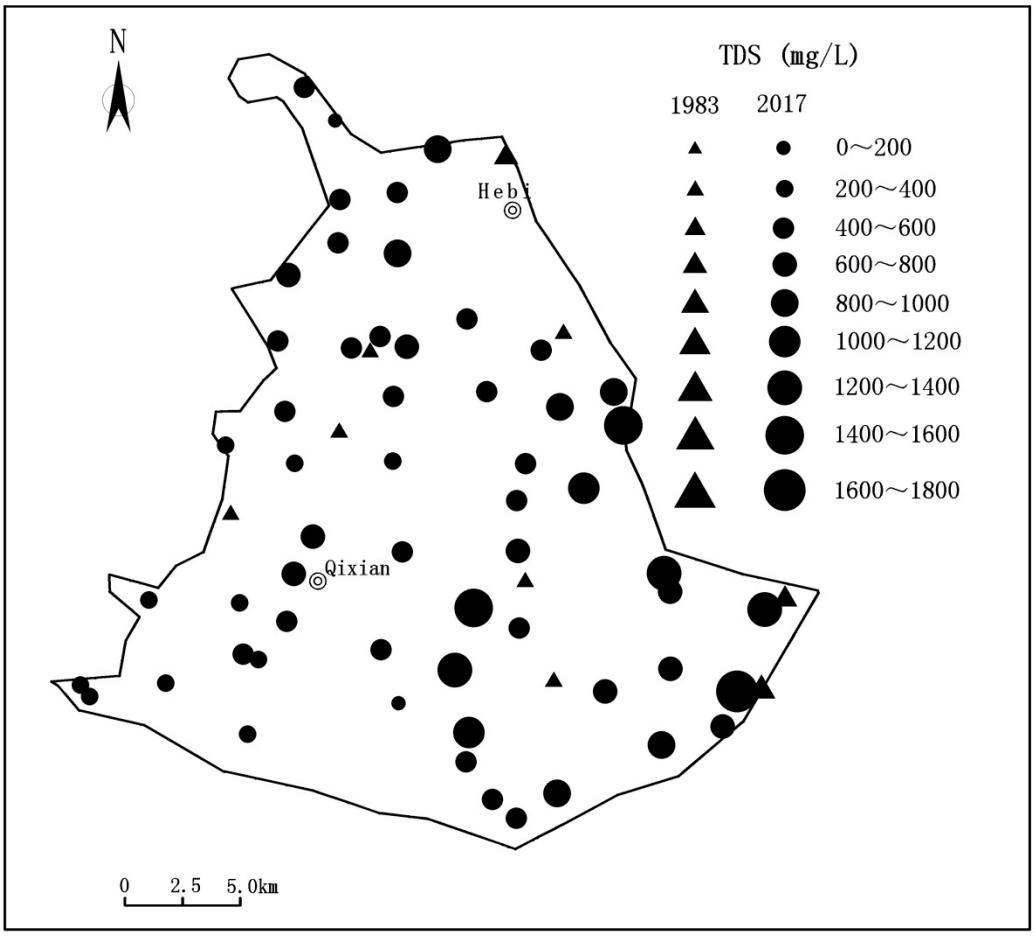


Fig. 4. Spatial pattern of total dissolved solids in groundwater.

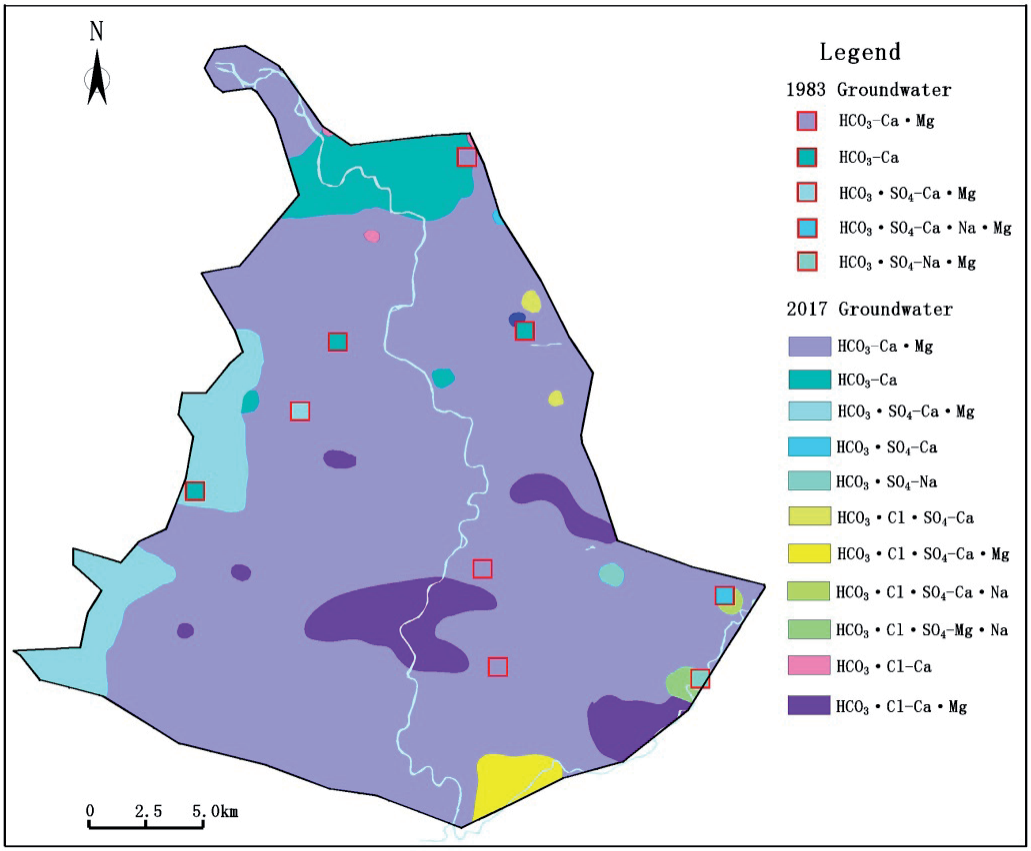


Fig. 5. Spatial pattern of hydrochemical types in groundwater of the QRAF.

Ca·Mg, HCO_3·SO_4-Ca·Na·Mg and HCO_3·SO_4-Na·Mg types were sporadically distributed in the western and southeastern parts of the study area.

In 2017, the dominant hydrochemical type of groundwater was still HCO_3-Ca·Mg, and the distribution range of HCO_3-Ca type moved to the north. In areas with a high concentration of chemical enterprises, the groundwater in the western slope-diluvial slope and the lower reaches of the Qihe River showed HCO_3·SO_4-Ca·Mg and HCO_3·Cl-Ca·Mg types, respectively. Meanwhile, groundwater types along the low-lying areas of the Weihe River were highly complex, with the distribution of HCO_3·Cl·SO_4-Ca·Mg, HCO_3·Cl·SO_4-Ca·Na, HCO_3·Cl·SO_4-Mg·Na and HCO_3·Cl-Ca·Mg types, which were likely influenced by sluggish groundwater flow, enhanced evaporation, and anthropogenic discharges into the Weihe River.

Controlling Factors of Water Chemistry

Water-rock Interaction

The Gibbs diagram method [35] provides a direct means of identifying the mechanisms that control groundwater hydrochemistry based on the relationships between the cation ratio $Na^+/(Na^+{+}Ca^{2+})$, the anion ratio $Cl^-/(Cl^-{+}HCO_3^-)$, and total dissolved solids (TDS). Commonly, the natural controlling factors can be classified into three categories: atmospheric precipitation, evaporation, and rock weathering [36-38]. As shown in Fig. 6, the $Na^+/(Na^+{+}Ca^{2+})$ ratio ranged from 0.09 to 0.72 in 1983 and from 0.07 to 0.77 in 2017, with average values of 0.29 and 0.19, respectively. $Cl^-/(Cl^-{+}HCO_3^-)$ ratios in 1983 and 2017 ranged from 0.04 to 0.25 and from 0.06 to 0.58, with average values of 0.12 and 0.21, respectively. These results suggest that the dominant source of groundwater solutes is water-rock interaction. However, several samples with $Na^+/(Na^+{+}Ca^{2+})$ values exceeding 0.6 fell outside the typical Gibbs diagram range in both periods, indicating that the chemical components in these areas may have been influenced by anthropogenic activities [39]. Moreover, in 2017, a greater number of groundwater samples shifted toward the "evaporation dominance" zone, due to higher evaporative concentration, indicating an increased influence of evaporation on groundwater chemistry over time.

An end-member mixing diagram [40] was employed to further assess the relative contributions of carbonate, silicate, and evaporite rock weathering [41]. As illustrated in Fig. 7, carbonate end-members have values of 50 for Ca^{2+}/Na^+, 10 for Mg^{2+}/Na^+, and 120 for HCO_3^-/Na^+, whereas silicate end-members have values of 0.35±0.15 for Ca^{2+}/Na^+, 0.24±0.12 for Mg^{2+}/Na^+, and 2±1 for HCO_3^-/Na^+. In the figure, samples of groundwater in 1983 and 2017 both plotted primarily between the two end-members of silicates and carbonates, indicating that

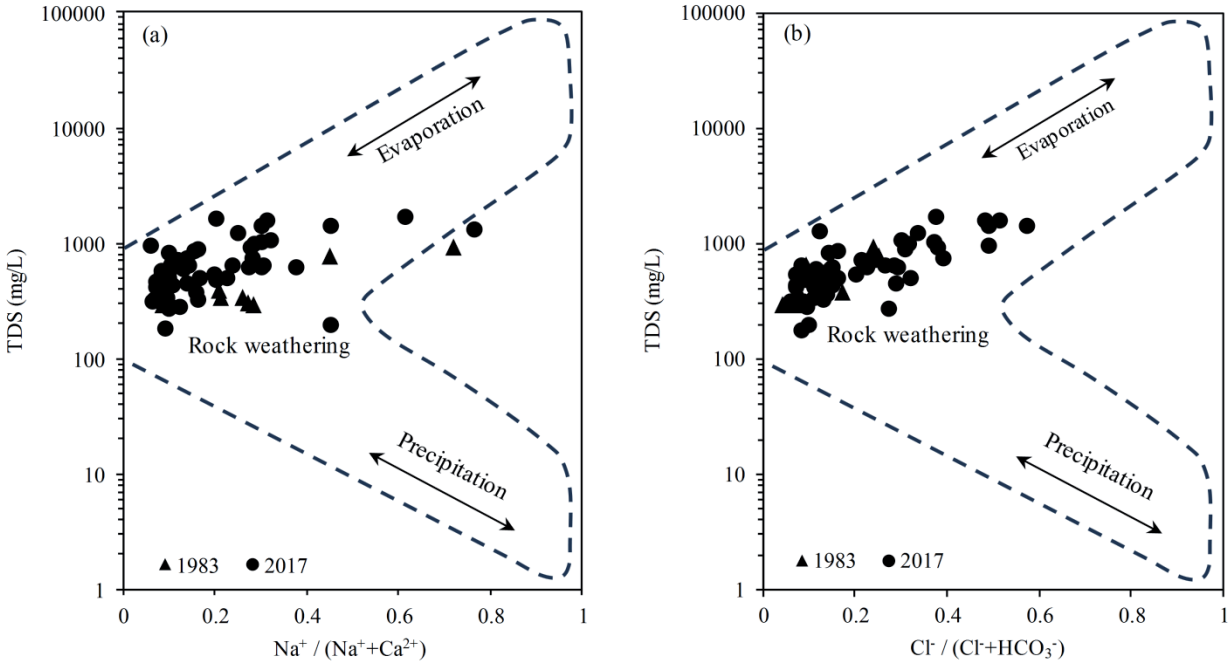


Fig. 6. Gibbs diagram of the groundwater samples.

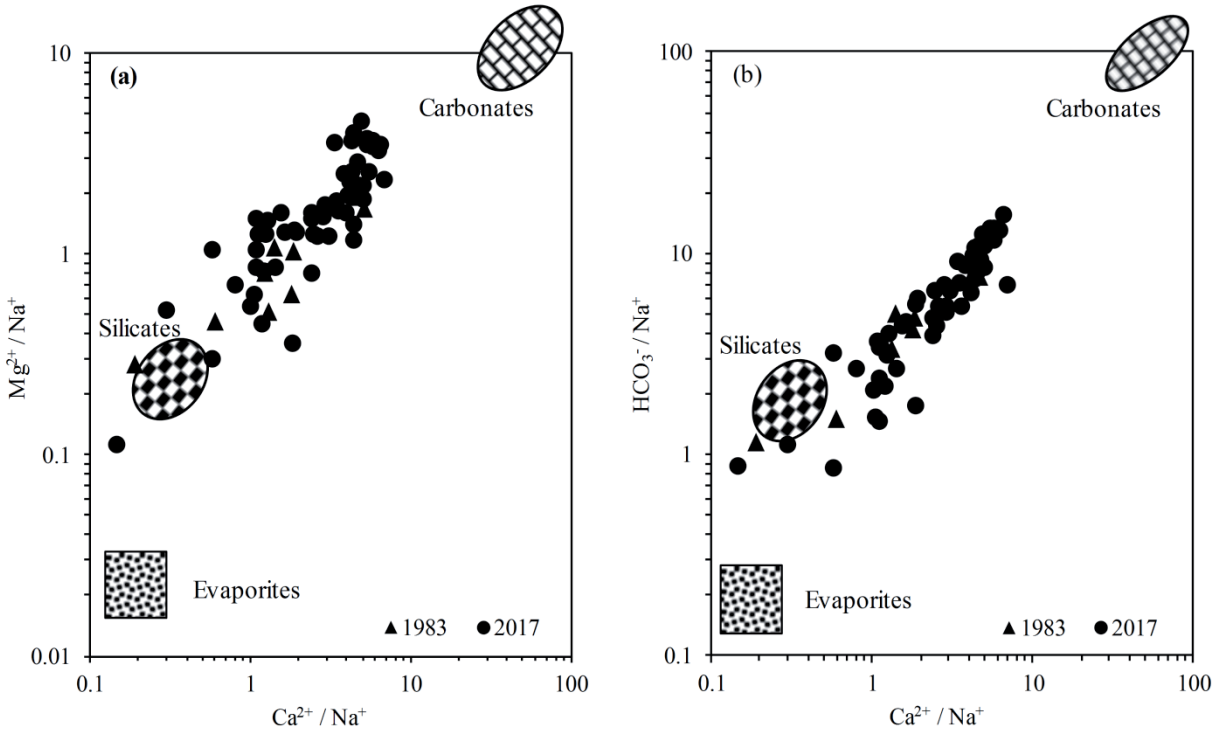


Fig. 7. End-member diagram of the groundwater samples in the QRAF.

the chemical composition of groundwater in the QRAF is primarily controlled by the weathering of silicate rocks and the dissolution of carbonate minerals.

Analysis of Chemical Control Factors of Groundwater

Based on correlation analysis and principal component analysis (PCA) [42], the hydrochemical characteristics of groundwater in the study area and their dominant controlling factors were analyzed, and the ion-association patterns and number of controlling factors differed significantly between the two periods (Fig. 8, Table 2). In 1983, the major ions (K^++Na^+, Mg^{2+}, Cl^-, SO_4^{2-}, and HCO_3^-) showed very strong positive correlations with TDS (r>0.8), indicating that the groundwater chemical composition during this

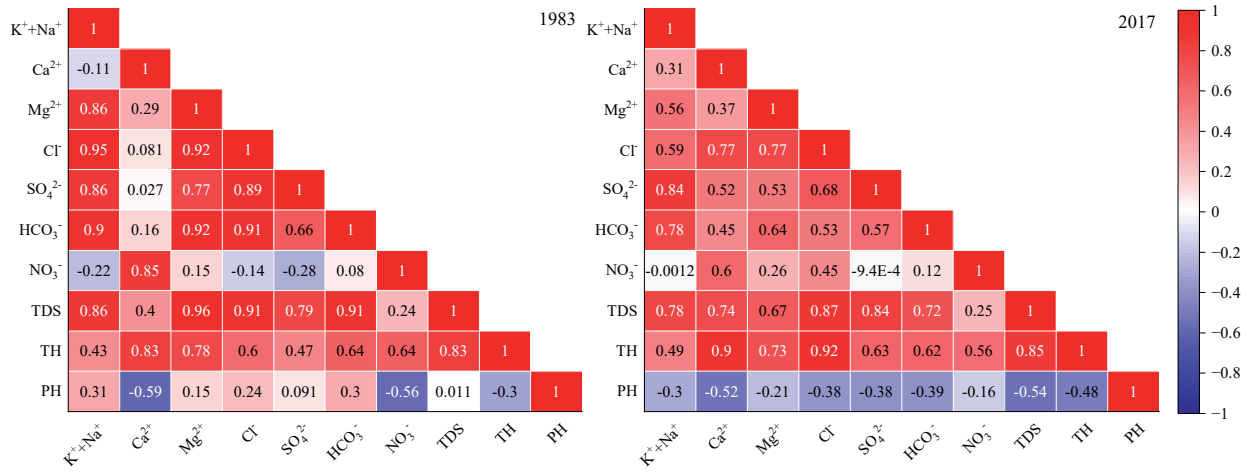


Fig. 8. Correlation coefficient matrix of hydrochemical parameters.

Table 2. Component matrix.

Year	Factor	K^++Na^+	Ca^{2+}	Mg^{2+}	Cl^-	SO_4^{2-}	HCO_3^-	NO_3^-	TDS	TH	pH
1983	F1	0.90	0.30	0.98	0.96	0.83	0.93	0.12	0.99	0.77	0.11
	F2	-0.37	0.92	0.01	-0.24	-0.27	-0.12	0.93	0.12	0.61	-0.76
2017	F1	0.92	0.30	0.76	0.67	0.84	0.80	-0.10	0.80	0.57	-0.20
	F2	-0.05	0.74	0.44	0.65	0.07	0.14	0.90	0.38	0.75	-0.16
	F3	0.16	0.51	-0.17	0.16	0.33	0.19	0.02	0.40	0.29	-0.89

period was mainly controlled by water-rock interaction, and that natural processes such as silicate/carbonate mineral weathering and evaporation concentration dominated ion migration and enrichment. By 2017, although these natural association patterns remained evident, stronger correlations emerged between Ca^{2+}, Mg^{2+}, Cl^-, and NO_3^-, reflecting the enhanced influence of human activities on the groundwater chemical composition.

The principal component analysis results showed that two principal components extracted for 1983 explained 88.98% of the total variance. Principal component 1 (PC1, 59.52%) was dominated by K^++Na^+, Mg^{2+}, Cl^-, SO_4^{2-}, HCO_3^-, and TDS (loadings>0.8), reflecting the dominant control of natural water-rock interaction. Principal component 2 (PC2, 29.46%) was dominated by Ca^{2+}, NO_3^-, and TH (loadings>0.6), indicating the influence of carbonate mineral dissolution and weak agricultural activity. In 2017, three principal components were required to explain 86.3% of the total variance, indicating a substantial increase in the complexity of controlling factors. Principal component 1 (PC1, 48.2%) was still mainly loaded by K^++Na^+, Mg^{2+}, Cl^-, SO_4^{2-}, HCO_3^-, and TDS, suggesting that water-rock interaction remained the dominant control. Principal component 2 (PC2, 25.1%) was jointly dominated by Ca^{2+}, Mg^{2+}, Cl^-, TH, and NO_3^-, reflecting the combined influence of carbonate weathering and anthropogenic pollution. The newly identified principal component 3 (PC3, 13.0%) was dominated by a strong negative loading of pH (-0.89) and showed moderate associations with Ca^{2+} and TDS, which may be related to increased regional CO_2 partial pressure, enhanced organic-matter decomposition, or acid-deposition input.

Solute Source Identification

Ion Ratio Analysis

Ion ratio analysis is a commonly used method to identify the sources of major ions and to further investigate the chemical evolution of groundwater [43, 44]. When halite dissolution is the dominant source of Na^+ and Cl^- in groundwater, the Na^+/Cl^- molar ratio is expected to approximate 1 (Eq. (2)). As shown in Fig. 9a), the average Na^+/Cl^- ratio decreased from 2.35 in 1983 to 1.01 in 2017, with a higher proportion of data points located above the y = x line in 1983 than in 2017. This suggests that the 1983 groundwater samples may have been influenced by halite dissolution, silicate weathering, and cation exchange processes, as depicted in Eqs. (3)-(5). In 2017, the sample points were distributed mainly on both sides of the y = x line, and the Cl^- equivalent concentration was significantly higher than that of Na^+ at some points, indicating that in addition to halite and silicate dissolution or

cation exchange, some water samples may also reflect anthropogenic influences [39].

The relationships among Mg^{2+}, Ca^{2+}, and HCO_3^- can help identify the role of carbonate mineral dissolution (e.g., dolomite and calcite) in controlling groundwater chemistry, as shown in Eqs. (6)- (9). As illustrated in Fig. 9b), the majority of the water sample points from 1983 and 2017 were above the y = x line, implying the dissolution of carbonates as a major source of Ca^{2+}, Mg^{2+}, and HCO_3^-. Further, the Ca/Mg ratio can reveal the type of dissolved carbonate rock, with ratios above the y = 2x line indicating calcite dominance, and ratios near the y = x line suggesting dolomite as the main source [45]. Fig. 9c) shows that the water points are scattered on both sides of the y = 2x line, and there are significantly more points below the y = 2x line than above it, indicating that dolomite is the predominant carbonate mineral contributing to groundwater chemistry, followed by calcite. At the same time, the ratio of Ca^{2+} to SO_4^{2-} in groundwater can be used to assess the dissolution of gypsum (Eq. (10)), a common accessory mineral in carbonate-rich regions [46]. As shown in Fig. 9d), the pattern in 1983 was similar to that in 2017. Most samples fell above the y = x line, indicating that the influence of Ca^{2+} from the dissolution of evaporite rocks is relatively minor.

The ratio of HCO_3^- to (SO_4^{2-} + Cl^-) offers insight into the relative influence of carbonate, silicate, and evaporite weathering on groundwater composition [47]. As depicted in Fig. 9e), most water sample points are located above the y = x line, with a minority below it. This indicates that the ions in groundwater are mainly affected by the dissolution of carbonate and silicate rocks, but little by the dissolution of evaporite rocks. Additionally, the scatter plots of Ca^{2+} + Mg^{2+} and SO_4^{2-} + HCO_3^- reflect the contributions of dissolution and/or precipitation of carbonate and silicate minerals to groundwater chemistry [48]. Fig. 9f) shows that the sample points in 2017 are mostly located above the y = x line, with a greater number of 1983 samples

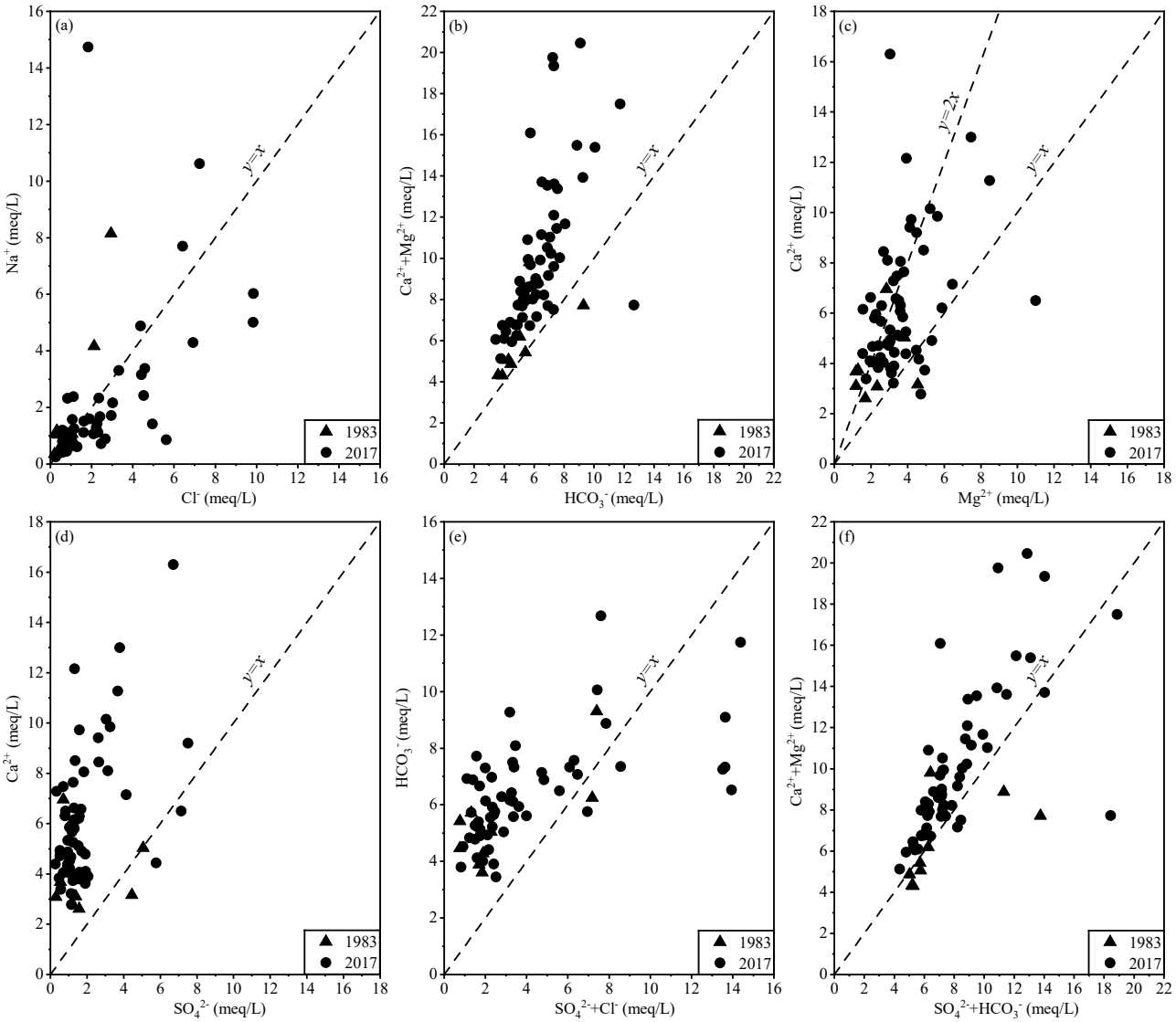


Fig. 9. Ion-ratio diagrams of groundwater chemical components in the study area.

falling below the line. This suggests that the water chemical characteristics are affected by the weathering of carbonates and silicates, suggesting that carbonate weathering played a more prominent role in 2017, whereas silicate weathering was more significant in 1983.

$$NaCl \rightarrow Na^+ + Cl^- \quad (2)$$

$$2NaAlSi_3O_8 + 2CO_2 + 11H_2O \rightarrow 2Na^+ + 2HCO_3^- + Al_2Si_2O_5(OH)_4 + 4H_4SiO_4 \quad (3)$$

$$\text{Forward: } Ca^{2+} + 2NaX \rightarrow 2Na^+ + CaX_2 \quad (4)$$

$$\text{Reverse: } 2Na^+ + CaX_2 \rightarrow Ca^{2+} + 2NaX \quad (5)$$

$$CaCO_3 + H^+ \rightarrow Ca^{2+} + HCO_3^- \quad (6)$$

$$CaCO_3 + H_2O + CO_2 \rightarrow Ca^{2+} + 2HCO_3^- \quad (7)$$

$$CaMg(CO_3)_2 + 2H^+ \rightarrow Ca^{2+} + Mg^{2+} + 2HCO_3^- \quad (8)$$

$$CaMg(CO_3)_2 + 2H_2O + 2CO_2 \rightarrow Ca^{2+} + Mg^{2+} + 4HCO_3^- \quad (9)$$

$$CaSO_4 \rightarrow Ca^{2+} + SO_4^{2-} \quad (10)$$

Cation Exchange

Cation exchange can significantly influence the chemical characteristics of groundwater in a region [49]. The relationship between $Ca^{2+} + Mg^{2+} - HCO_3^- - SO_4^{2-}$ and $Na^+ + K^+ - Cl^-$ is commonly used to assess the occurrence and intensity of the cation exchange process. As shown in Fig. 10a), most groundwater samples plot near the y = -x line, confirming that cation exchange plays an important role in shaping groundwater hydrochemistry [50]. According to Fig. 10a), groundwater sample points fall near the y = -x line, confirming the existence of cation exchange adsorption. Furthermore, the direction of cation exchange can be inferred from the chlor-alkali indices (CAIs) [51], which are calculated using Eqs. (11) and (12).

$$CAI\text{-}1 = \frac{Cl^- - (Na^+ + K^+)}{Cl^-} \quad (11)$$

$$CAI\text{-}2 = \frac{Cl^- - (Na^+ + K^+)}{HCO_3^- + SO_4^{2-} + CO_3^{2-} + NO_3^-} \quad (12)$$

Positive values of CAI-1 and CAI-2 indicate reverse ion exchange, where sodium in groundwater replaces calcium adsorbed onto the aquifer matrix. Conversely, negative values imply forward ion exchange, in which calcium in groundwater is exchanged for sodium from the matrix [52, 53]. Fig. 10b) demonstrates that most water sample points from 1983 and 2017 were located in zone I and zone II, respectively, indicating that forward cation exchange prevailed in 1983 and shifted towards reverse exchange in 2017.

The alluvial-proluvial fan strata in the study area consist, from north to south, of limestone, siltstone, and interbedded clayey sandstone. Calcareous nodules and clay minerals are widely developed in the vadose zone and aquifer media, providing stable material carriers

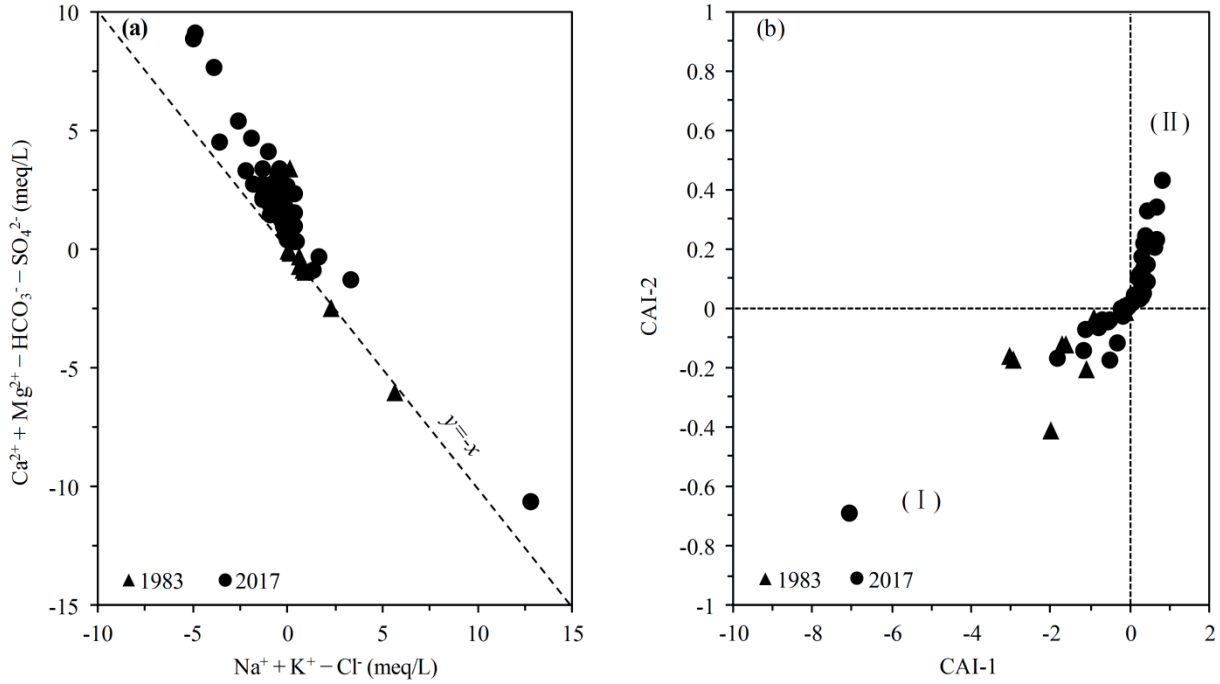


Fig. 10. Plots of a) $(Na^+ + K^+ - Cl^-)$ vs $(Ca^{2+} + Mg^{2+} - HCO_3^- - SO_4^{2-})$, b) CAI-1 vs CAI-2.

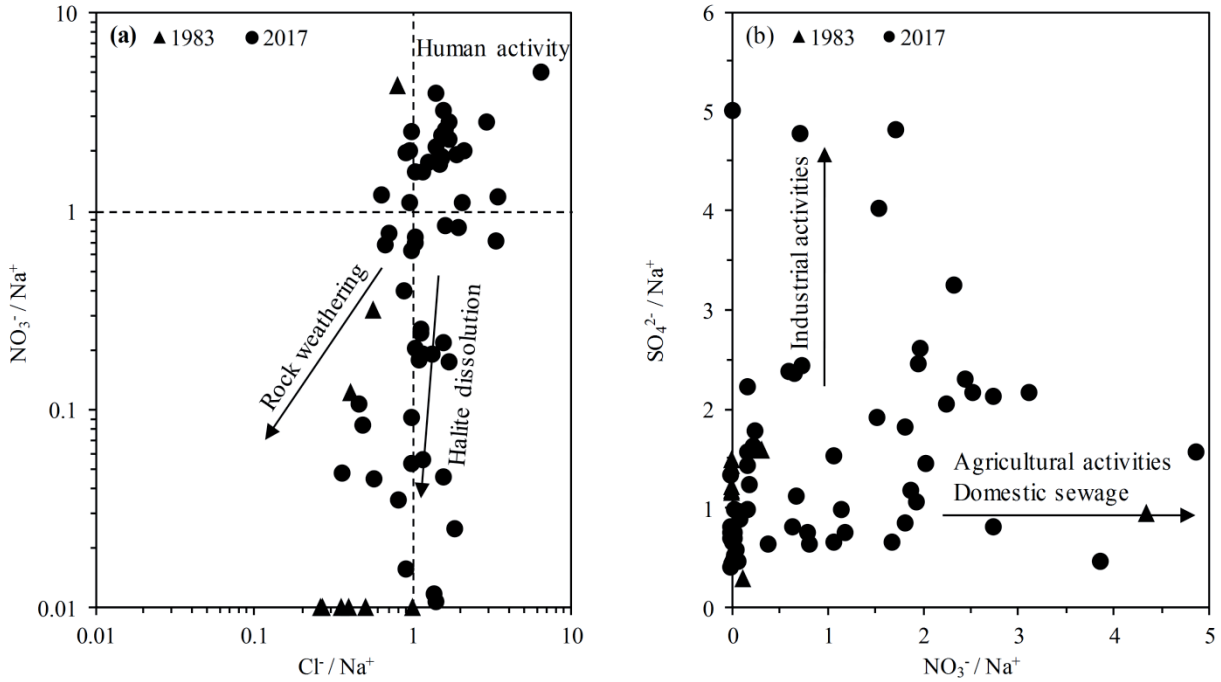


Fig. 11. Ion ratio relationships for identifying human activities in groundwater.

and reaction interfaces for Ca-Na cation exchange. The exchange direction is mainly controlled by the relative activity of ions in the aqueous phase and the equilibrium of competitive adsorption. In 1983, groundwater chemistry was dominated by natural water-rock interaction, and the ionic system was relatively simple. The competitive adsorption capacity of divalent cations was dominant, leading to forward cation exchange. By 2017, under the influence of human activities, the ionic strength of groundwater had increased significantly, the activity coefficients of divalent cations had decreased, and their competitive advantage had been weakened. Meanwhile, the relative activity and adsorption competitiveness of Na^+ increased, and the exchange direction gradually shifted toward reverse cation exchange. This also reflects, to some extent, the restructuring of hydrogeochemical equilibrium under anthropogenic disturbance.

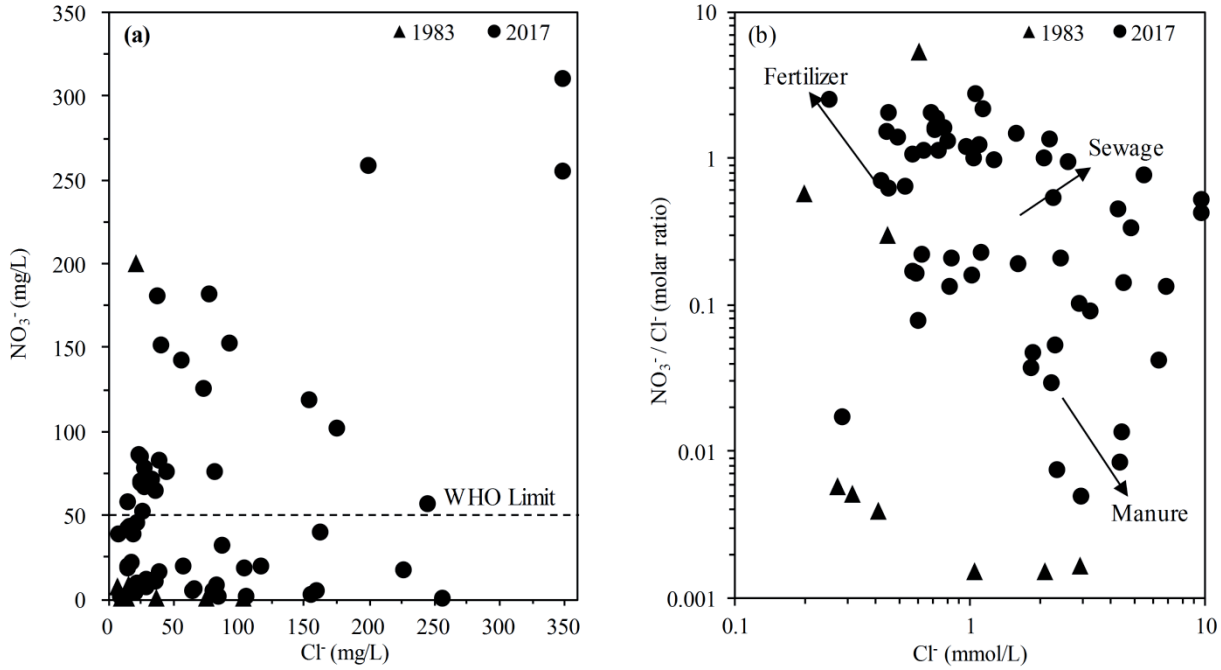


Fig. 12. Plots of a) NO_3^- vs Cl^-, b) NO_3^-/Cl^- vs Cl^-.

Human Activities

With the advancement of socio-economic development, human activities have become a major factor affecting groundwater chemistry, primarily reflected by elevated concentrations of NO_3^-, Cl^- and SO_4^{2-} [54]. NO_3^- and Cl^- typically originate from domestic sewage and agricultural fertilizer application, while SO_4^{2-} is mainly derived from industrial effluents and mining activities. In general, groundwater impacted by anthropogenic activities exhibits elevated NO_3^-/Na^+ and Cl^-/Na^+ ratios [41, 55]. Fig. 11a) shows that the majority of water samples from 1983 and 2017 are in the "rock weathering" and "halite dissolution" zones, while several 2017 samples fall within the "human activity" domain, indicating anthropogenic influence. This indicates that the composition of groundwater in 1983 was generally influenced by rock weathering and halite dissolution, while the groundwater in 2017 was influenced by rock weathering, halite dissolution and human activities. The relationship between SO_4^{2-}/Na^+ and NO_3^-/Na^+ ratios provides valuable insight into the type and extent of anthropogenic influence on groundwater chemistry [41]. A high SO_4^{2-}/Na^+ ratio coupled with a low NO_3^-/Na^+ ratio suggests predominant influence from industrial sources, whereas the opposite pattern indicates impacts from agricultural and domestic sources [56]. As shown in Fig. 11b), the two ratios in groundwater in 2017 show a positive correlation, suggesting that the hydrochemical evolution of groundwater in 2017 is likely driven by a combination of industrial activities, agriculture, and domestic wastewater. In contrast, both ratios in groundwater in 1983 are low, further confirming that groundwater in 1983 was comparatively less influenced by anthropogenic inputs.

Fig. 12a) shows that 43.9 % of groundwater samples in 2017 and only one sample in 1983 exceeded the nitrate concentration limit (50 mg/L) recommended by the WHO. This indicates that shallow groundwater was more significantly polluted in 2017 compared to 1983. In addition, most of the groundwater samples in 2017 were characterized by fairly high Cl^- values, and NO_3^- showed a significant correlation with Cl^-, indicating that both ions may originate from the same anthropogenic sources. The relation between the NO_3^-/Cl^- ratio and Cl^- concentration provides valuable insight into the sources of NO_3^- and Cl^- in water [57, 58]. As shown in Fig. 12b), a few samples collected in 1983 were plotted in the fertilizer-dominated zone, suggesting that nitrate primarily originated from agricultural activities. Most samples collected in 2017 were mainly plotted in the zone dominated by fertilizer and sewage inputs. This suggests that nitrate in 2017 originated from both agricultural activities and domestic sewage.

Conclusions

In order to understand the effects of natural and human factors on the chemical composition of groundwater in the process of rapid urbanization, mathematical statistics, Shukarev classification, the Gibbs model, and ion-ratio analysis were applied to analyze the ion characteristics and evolution mechanism of shallow groundwater in the QRAF at the southern edge of the Taihang Mountains. The research results indicate that the abundance of major cations was in the order of $Ca^{2+}>Na^+>Mg^{2+}>K^+$, while the major anions followed the order: $HCO_3^->SO_4^{2-}>Cl^->NO_3^-$. From 1983 to 2017, the total cation concentration, total anion concentration, TDS and TH of the shallow groundwater in the QRAF showed an upward trend over time. The average concentration of NO_3^- increased significantly in 2017, with a coefficient of variation of 1.15, and 43.9 % of groundwater samples exceeded the permissible limit proposed by the WHO, indicating a strong influence of human activities on groundwater quality. HCO_3-Ca and HCO_3-Ca·Mg water types remained the predominant hydrochemical facies, but the distribution range of HCO_3-Ca had moved northward by 2017, and under the influence of slow groundwater runoff, increased evaporation and anthropogenic drainage to the Weihe River, the groundwater chemical types in the low-lying land along the Weihe River became very complex.

The main mechanism regulating groundwater chemistry was determined to be rock weathering, and major groundwater ions originated from the dissolution of silicate and carbonate minerals, with carbonate weathering in 2017 and silicate weathering in 1983 being dominant. In addition, cation exchange was recognized as a crucial hydrogeochemical process that also influenced the chemical composition of groundwater, with forward cation exchange occurring in 1983 and then gradually shifting to reverse cation exchange in 2017. Groundwater in the study area gradually shifted from an early, relatively simple evolutionary pattern dominated by natural processes such as water-rock interaction to a complex evolutionary pattern jointly controlled by natural processes, anthropogenic inputs, and changes in the acid-base environment. In 2017, anthropogenic inputs, including industrial activities, agricultural activities, and domestic sewage, exerted a stronger influence on groundwater chemical evolution, with NO_3^- mainly derived from agricultural activities and domestic sewage.

Acknowledgements

This work was supported by the Open Fund for Hebei Province Collaborative Innovation Center for Sustainable Utilization of Water Resources and Optimization of Industrial Structure (SXTCX202504), the Investigation Project of China Geological Survey

(DD20251242, DD20160310), and the State Key Laboratory of Biogeography and Environmental Geology (GBL22110). Meanwhile, we thank the anonymous reviewers and Editor for their insightful comments and suggestions, which helped improve the manuscript.

AI Usage Disclosure Statement

The authors confirm that no generative artificial intelligence tools were used in the research or in the preparation, translation, language editing, or submission of this manuscript.

Conflict of Interest

The authors declare no conflict of interest.

References

1. ROHDE M.M., ALBANO C.M., HUGGINS X., KLAUSMEYER K.R., MORTON C., SHARMAN A., ZAVERI E., SAITO L., FREED Z., HOWARD J.K., JOB N., RICHTER H., TODERICH K., RODELLA A.-S., GLEESON T., HUNTINGTON J., CHANDANPURKAR H.A., PURDY A.J., FAMIGLIETTI J.S., SINGER M.B., ROBERTS D.A., CAYLOR K., STELLA J.C. Groundwater-dependent ecosystem map exposes global dryland protection needs. Nature, **632** (8023), 101, **2024**.
2. LAPWORTH D.J., BOVING T.B., KREAMER D.K., KEBEDE S., SMEDLEY P.L. Groundwater quality: Global threats, opportunities and realising the potential of groundwater. Science of The Total Environment, **811**, 152471, **2022**.
3. GLEESON T., WADA Y., BIERKENS M.F.P., VAN BEEK L.P.H. Water balance of global aquifers revealed by groundwater footprint. Nature, **488** (7410), 197, **2012**.
4. SHARMA C., BAŞAĞAOĞLU H., YOOSEFDOOST I., WOOTTEN A., CHAKRABORTY-REDDY D., BERTETTI F.P., MIRCHI A., CHAKRABORTY D. Efficacy of mitigation strategies for aquifer sustainability under climate change. Nature Sustainability, **8** (1), 44, **2024**.
5. KHODJA H.D., AICHOUR A., METAICHE M., FERHATI A. Hydrochemical Assessment of Albian Waters of Southern Algeria Using Water Quality Indices. Polish Journal of Environmental Studies, **34** (5), 5599, **2025**.
6. XIAO Y., LIU K., HAO Q., XIAO D., ZHU Y., YIN S., ZHANG Y. Hydrogeochemical insights into the signatures, genesis and sustainable perspective of nitrate enriched groundwater in the piedmont of Hutuo watershed, China. Catena, **212**, **2022**.
7. ABDELBAKI H., BELKENDIL A., MAAZOUZI A., MEKKAOUI A. Assessment of hydrochemical properties of groundwater in the alluvial aquifer of the arid zone of the Igli Region, South-West of Algeria. Desalination and Water Treatment, **268**, 153, **2022**.
8. HOU X., WANG W., WANG Z., MA Z., GUAN C., XI D., LI P., LI J., HUANG X. Hydrogeological processes and hydrochemical effects in the Manas river catchment, Northwest China, over the past 60 years. Journal of Hydrology, **614** (Part A), **2022**.
9. BARATHKUMAR S., SELLAMUTHU K.M., SATHIYABAMA K., MALATHI P., KUMARAPERUMAL R., DEVAGI P., PAZHANIVELAN S. Groundwater quality assessment in selected polluted hotspots of Tamil Nadu, India using geospatial and statistical approaches. Desalination and Water Treatment, **322**, 101047, **2025**.
10. SIDAURUK P., PRASETIO R., SATRIO, PUJIINDIYATI E.R. Origin and recharge area determination of springs around a lake for sustainability of the lake. Journal of Human, Earth, and Future, **6** (1), 27, **2025**.
11. CHEN L., FENG Q. Geostatistical analysis of temporal and spatial variations in groundwater levels and quality in the Minqin oasis, Northwest China. Environmental Earth Sciences, **70** (3), 1367, **2013**.
12. WANG J., GE Z., XIA R., HE S., ZHAN S. Hydrogeochemistry and stable isotopes of water: Characteristics, influencing factors and sources in a semi-arid irrigated basin, Hetao Plain. Journal of Arid Environments, **227**, **2025**.
13. ZHAO Z., GAO Z., LIU J., LUO Z., SUN H., WANG Y., LI F. Hydrochemical characterization and comprehensive water quality assessment of groundwater within the main stream area of Yishu River. Environmental Monitoring and Assessment, **196** (6), **2024**.
14. WANG Z., WANG Y., SHI M., JI W., LI R., WANG X. Coordinated analysis of groundwater spatiotemporal chemical characteristics, water quality, and potential human health risks with sustainable development in semi-arid regions. Environmental Geochemistry and Health, **46** (10), 370, **2024**.
15. HE B., HE J., ZENG Y., SUN J., PENG C., BI E. Coupling of multi-hydrochemical and statistical methods for identifying apparent background levels of major components and anthropogenic anomalous activities in shallow groundwater of the Liujiang Basin, China. Science of The Total Environment, **838**, 155905, **2022**.
16. HAN D., CURRELL M.J., GUO H. Controls on distributions of sulphate, fluoride, and salinity in aquitard porewater from the North China Plain: Long-term implications for groundwater quality. Journal of Hydrology, **603**, 126828, **2021**.
17. XING L., GUO H., ZHAN Y. Groundwater hydrochemical characteristics and processes along flow paths in the North China Plain. Journal of Asian Earth Sciences, **70-71**, 250, **2013**.
18. LI C., GAO Z., CHEN H., WANG J., LIU J., LI C., TENG Y., LIU C., XU C. Hydrochemical analysis and quality assessment of groundwater in southeast North China Plain using hydrochemical, entropy-weight water quality index, and GIS techniques. Environmental Earth Sciences, **80** (16), **2021**.
19. GU X., XIAO Y., YIN S., PAN X., NIU Y., SHAO J., CUI Y., ZHANG Q., HAO Q. Natural and anthropogenic factors affecting the shallow groundwater quality in a typical irrigation area with reclaimed water, North China Plain. Environmental Monitoring & Assessment, **189** (10), 514, **2017**.
20. GUO X., WANG W., SHI J., CHEN Z., GUO J., WANG H., LIU W., MIAO Y. Hydrochemical evolution and hydrological zoning characteristics of a shallow groundwater system in Baiyangdian Wetland, North China Plain. Hydrological Processes, **38** (6), e15219, **2024**.

21. YANG Y., ZHANG Z., WANG Z., LIU H., SUN Z. Formation of high fluoride groundwater and associated health risks in the Cangzhou area of the North China Plain. Environmental Earth Sciences, **84** (4), 111, **2025**.
22. LIU J., TSUJIMURA M., ZHANG J., YI Z. Utilizing Stable Isotopes and Major Ions to Isolate the Recharge Regime of an Alluvial-Proluvial Fan Aquifer in the Piedmont Region of the South Taihang Mountains, North China Plain. Water Resources, **50** (6), 969, **2023**.
23. HUANG X.-Y., ZHANG D., ZHAO Z.-Q., LIU Y.-T., MENG H.-Q., ZOU S., MA B.-J., FENG Q.-Y. Determining hydrogeological and anthropogenic controls on N pollution in groundwater beneath piedmont alluvial fans using multi-isotope data. Journal of Geochemical Exploration, **229**, **2021**.
24. ZHANG Q., WANG L., WANG H., ZHU X., WANG L. Spatio-Temporal Variation of Groundwater Quality and Source Apportionment Using Multivariate Statistical Techniques for the Hutuo River Alluvial-Pluvial Fan, China. International Journal of Environmental Research and Public Health, **17** (3), 1055, **2020**.
25. QIU Y., MA C., QIAN J., WANG X. Comparison of different groundwater vulnerability evaluation models of typical karst areas in north China: a case of Hebi City. Environmental Science and Pollution Research, **28** (24), 30821, **2021**.
26. LI P., WU J., QIAN H. Hydrogeochemistry and quality assessment of shallow groundwater in the southern part of the Yellow River alluvial plain (Zhongwei section), Northwest China. Earth Sciences Research Journal, **18** (1), 27, **2014**.
27. CHEN K., LIU Q., PENG W., LIU X. Source apportionment and natural background levels of major ions in shallow groundwater using multivariate statistical method: A case study in Huaibei Plain, China. Journal of Environmental Management, **301**, 113806, **2022**.
28. LIU J., LOU K., GAO Z., TAN M. Hydrochemical insights on the signatures and genesis of water resources in a high-altitude city on the Qinghai-Xizang Plateau, South-west China. Frontiers of Environmental Science & Engineering, **18** (7), **2024**.
29. LIU J., GAO Z., FENG J., WANG M. Identification of the hydrochemical features, genesis, water quality and potential health hazards of groundwater in Dawen River Basin, North China. Ecological Indicators, **149**, 110175, **2023**.
30. NIYAZI B. Groundwater assessment for sustainable development in the Wadi Al-Hamd Basin, Al-Madinah Al-Munawarah, KSA. Journal of African Earth Sciences, **215** (1), 105289, **2024**.
31. LI H., ZHANG W., WANG Y., ZHANG L., LI X., GENG H., LU Y. Chemical characteristics and evolution of groundwater in northeastern margin of the Tibetan Plateau, China. Environmental Geochemistry and Health, **47** (1), **2024**.
32. RADHI N.A., AL-MADHHACHI A.-S.T., SACHIT D.E. Groundwater quality and irrigation suitability assessment using geochemical and GIS-based approaches in arid regions. Civil Engineering Journal, **11** (11), 4536, **2025**.
33. TANG R., DONG S., ZHANG M., ZHOU Z., ZHANG C., LI P., BAI M. Hydrochemical Characteristics and Water Quality of Shallow Groundwater in Desert Area of Kunyu City, Southern Margin of Tarim Basin, China. Water, **15** (8), 1563, **2023**.
34. GUO P., CHEN S., LUO X., HU K., LI B. Hydrochemical Controlling Factors and Spatial Distribution Characteristics of Shallow Groundwater in Agricultural Regions of Central-Eastern Henan Province, China. Water, **17** (19), 2815, **2025**.
35. GIBBS R.J. Mechanisms controlling world water chemistry. Science, **170** (3962), 1088, **1970**.
36. SUBRAMANIYAN A., BALAJI A., ANDIMUTHU R. Assessment of groundwater quality for drinking and irrigation in Dindigul district, southern India: Hydrochemical characterization and spatial analysis. Desalination and Water Treatment, **320**, **2024**.
37. LU L., WANG Z., WANG Z., DENG L., ZOU S., FAN L., YANG Y. Chemical characteristics and water quality assessment of groundwater in the Dongjiang-Hanjiang River Basin, China. Journal of Environmental Chemical Engineering, **12** (6), **2024**.
38. DENG Y., LU Y., DU X., YE X., FENG J. Identifying spatial patterns and driving factors of anthropogenic impacts on the groundwater environment based on groundwater chemical kinetics. Journal of Cleaner Production, **486** (4), 144436, **2025**.
39. LI C., MEN B.-H., YIN S.-Y. Analysis of Groundwater Chemical Characteristics and Spatiotemporal Evolution Trends of Influencing Factors in Southern Beijing Plain. Frontiers in Environmental Science, **10**, **2022**.
40. GAILLARDET J., DUPRÉ B., LOUVAT P., ALLÈGRE C.J. Global silicate weathering and CO_2 consumption rates deduced from the chemistry of large rivers. Chemical Geology, **159** (1-4), 3, **1999**.
41. AN R., LIU J., GAO Z., LI C., PENG Y. Hydrochemical Characterization, Controlling Factors and Water Quality of Surface Water in Shandong Province, North China. Journal of Earth Science, **35** (1), 155, **2024**.
42. ABDELAZIZ S., KHEIMI M., EIZELDIN M.A.H., SAFI AHMED H. A comparative study of PCA and KPCA for groundwater quality index estimation. Civil Engineering Journal, **11** (11), 4453, **2025**.
43. FU C., LI X., CHENG X., LIU C., BAI Z., LI J. Hydrochemical processes and water balance trends based on stable isotopes of typical alpine lakes in the Qinghai-Tibet Plateau. Journal of Geochemical Exploration, **270**, **2025**.
44. WU Z., WU Y., YU Y., WANG L., QI P., SUN Y., FU Q., ZHANG G. Assessment of groundwater quality variation characteristics and influencing factors in an intensified agricultural area: An integrated hydrochemical and machine learning approach. Journal of Environmental Management, **371**, 123233, **2024**.
45. GUO Y., ZHANG C., XIAO Q., BU H. Hydrogeochemical characteristics of a closed karst groundwater basin in North China. Journal of Radioanalytical and Nuclear Chemistry, **325** (2), 365, **2020**.
46. JU Q., HU Y., LIU Q., CHEN K. Spatial and Temporal Evolutions of Shallow Groundwater with Anthropogenic Activities: A Case Study of Sunan Mine Region, China. Polish Journal of Environmental Studies, **33** (3), 2715, **2024**.
47. ZHANG T., WANG P., HE J., LIU D., WANG M., WANG M., XIA S. Hydrochemical Characteristics, Water Quality, and Evolution of Groundwater in Northeast China. Water, **15** (14), 2669, **2023**.
48. PAN X., SUN B., ZHANG S., LI G., TIAN Z., GUO Z., YU H., YANG Z. Ion sources and seasonal recharge characteristics of groundwater around Dali Lake in semi-arid region of Inner Mongolia Plateau, China. Journal of Geochemical Exploration, **269**, **2025**.

49. LIU J., PENG Y., LI C., GAO Z., CHEN S. Characterization of the hydrochemistry of water resources of the Weibei Plain, Northern China, as well as an assessment of the risk of high groundwater nitrate levels to human health. Environmental Pollution, **268**, **2021**.
50. XIAOTONG W., MENG C., YONG W., RENMAO Y., JINQIAN Y. Hydrogeochemical Characteristics and Evolution Processes of Multilayer Karst Aquifer in the Huayingshan Coalfield, Southwest China. Water Resources, **51** (4), 576, **2024**.
51. KRISHAN G., KUMAR M., RAO M.S., GARG R., YADAV B.K., KANSAL M.L., SINGH S., BRADLEY A., MUSTE M., SHARMA L.M. Integrated approach for the investigation of groundwater quality through hydrochemistry and water quality index (WQI). Urban Climate, **47**, **2023**.
52. HAJ R.A., MERHEB M., HALWANI J., OUDDANE B. Baseline hydro-geochemical characteristics of groundwater in Abu Ali watershed (Northern Lebanon). Journal of Hydrology: Regional Studies, **57**, 102135, **2025**.
53. YU Y., YAN B., TUO Y., ZHAN X., XIE X. Chemical evolution characteristics and influencing factors of groundwater in the saline and fresh water funnel area in Hengshui City, North China. Scientific Reports, **15** (1), **2025**.
54. GAO M., LI X., QIAN J., WANG Z., HOU X., GUI C., BAI Z., FU C., LI J., ZUO X. Hydrochemical Characteristics and Controlling Factors of Shallow and Deep Groundwater in the Heilongdong Spring Basin, Northern China. Sustainability, **15** (21), 15447, **2023**.
55. LIU J., LOU K., GAO Z., WANG Y., LI Q., TAN M. Comprehending hydrochemical fingerprint, spatial patterns, and driving forces of groundwater in a topical coastal plain of Northern China based on hydrochemical and isotopic evaluations. Journal of Cleaner Production, **461**, **2024**.
56. ZHANG M.-H., ZHOU S.-Y., LIU D.-D., ZHANG Y., ZHANG Y.-X., CHEN X., WANG H.-W., LI B., KANG W., YI B., SHI W.-P. Characteristics and genesis of groundwater salinization in coastal areas of the Lower Reaches of Oujiang Basin. Journal of Groundwater Science and Engineering, **12** (2), 190, **2024**.
57. XIA Y., LI Y., ZHANG X., YAN X. Nitrate source apportionment using a combined dual isotope, chemical and bacterial property, and Bayesian model approach in river systems. Journal of Geophysical Research: Biogeosciences, **122** (1), 2, **2017**.
58. SU C., LIU Y., CHENG Z., WANG W., ZHENG Z. Hydrochemical process and controls on the hydrochemistry of river water in the Muling-Xingkai Plain, Northeast China. Frontiers in Environmental Science, **10**, **2022**.